Liquefaction Identification Using IRS-1D Temporal Indices Data By Soft Computing Approach

S.S. Sengar, S.K. Ghosh & H.R. Wason
Indian Institute of Technology, Roorkee, India

A. Kumar*
Indian Institute of Remote Sensing, Dehradun, India

SUMMARY:

The M_w7.6 Bhuj earthquake that shook the Indian Province of Gujarat on the morning of January 26, 2001 was the most deadly in India's recorded history. Widespread appearance of soil liquefaction in the Rann of Kachchh and the coastal areas of Kandla port covering an area of tens of thousands of kilometers. Remote sensing products allow us to explore the land surface parameters at different spatial scales. This work is an attempt to document and identify the impact of using conventional band ratio indices from IRS-1D temporal images for liquefaction extraction was empirically investigated and compared with Class Based Sensor Independent (CBSI) spectral NDVI band ratio while applying possibilistic fuzzy classification as soft computing approach via supervised classification. It is found that CBSI temporal indices data approach was good for extraction liquefaction as well as water bodies.

Key words: *Indices, Liquefaction, Possibilistic c mean (PCM) classifier, Entropy, CBSI*

1. INTRODUCTION

The Bhuj area (Figure 1) has witnessed several hundreds of earthquakes from the historical period to this date (Malik et al., 1999). This earthquake was characterized by widespread liquefaction that caused sand volcanoes, ground cracking, lateral spreading of embankments, and water spouts over an area of more than 15,000 sq. km in the Rann of Kachchh. Liquefaction is a soil behavior phenomenon in which a saturated soil looses a substantial amount of strength due to high pore-water pressure generated by and accumulated during strong earthquake ground shaking. This work pertains to mapping the areas that showed sudden increase in soil moisture after the seismic event, using remote sensing technique. The basic principle behind using the satellite images in mapping the liquefaction changes is that electromagnetic spectrum absorbed by liquefied soil. Detailed information about how individual elements in a scene reflect or emit electromagnetic energy increases the probability of finding unique characteristics for a given element which allows for better distinction from other elements in the scene.

Digital image classification is a fundamental image processing operation to extract land cover information from remote sensing data and it assigns a class membership for each pixel in an image. Often, particularly in coarse spatial resolution images, the pixels may be mixed containing two or more classes. In conventional approach for extracting land cover classes; all the classes present in the area have to be identified first and then single class of interest can be taken out from the classified data. Soft computing approach handles vagueness, incomplete uncertain data. At this juncture, the principal constituents of Soft Computing (SC) are Fuzzy Logic (FL), Neural Computing (NC), Evolutionary Computation (EC) Machine Learning (ML) and Probabilistic Reasoning (PR), with the latter subsuming belief networks, chaos theory and parts of learning theory. For this reason it has been proposed that fuzziness should be accommodated in the

*Corresponding author anil@iirs.gov.in

classification procedure so that pixels may have multiple or partial class membership (Foody et al. 1996). Fuzzy approaches may be applied as supervised and unsupervised classification approaches.

Until recently many researchers in remote sensing field have applied useful classifications, such as Baraldi and Parmiggiani (1995) and Arora *et al*. (2004) use neural network, Bastin (1997) use fuzzy C-means, Pal and Mather (2003) use decision tree, Matsakis (2000) use fuzzy partitions, Wardlow and Egbert (2008) and Hansen *et al*. (2000) used NDVI data, Lucas *et al*. (2007), used time series remote sensing data for specific land use/land cover (LULC) identification. Gupta *et al.* (1998), Ramakrishnan *et al*. (2006) and Saraf *et al*. (2002) successfully demonstrated the application of remote sensing technique to map the earthquake induced liquefaction around the Bhuj. These methods help in mapping the liquefaction accurately. However, while going through the literature it has been identified that to find liquefaction using various indices with possibilistic fuzzy classifier has not been explored in the past. In this study it has been tried to identify liquefaction using temporal indices.

2. INDICES AND CLASSIFICATION APPROACHES

For generating band ratio data, it is important to know various types of band information present in multi-spectral data. Based on spectral information of remote sensing data, the user has to decide which spectral bands of data are to be used in different band ratio functions and require expert knowledge.

2.1 CBSI Spectral Band Ratio

To overcome the need for expert knowledge about remote sensing data, in this work a CBSI spectral band ratio has been proposed in Eqn. 2.1;

$$\text{CBSI band ratio} = min, max^{f\{(g_{1\ldots\ldots n})_{r,c}\}}\text{k} \tag{2.1}$$

where; g is grey value, r and c are row and column of a class location respectively, n denotes number of bands, k denotes number of classes. In Eqn. 2.1 user has to provide the location of a class in the form of row and column or latitude and longitude. At the class of interest (liquefaction) location, spectral information as grey value from all the bands will be read. While applying minimum, maximum operators to find out which band has minimum and which has maximum gray values. Then the band having maximum value is denoted as NIR and band having minimum values as Red in different indices. Here a simple condition is also applied that if indices values were negative then replace it with zero value. This enhances the concerned class of interest and only requires geo-location of a class, while spectral remote sensing data information is not required. Rouse *et al*. (1973) suggested the most widely used Normalized Difference Vegetation Index (NDVI) to improve identifying the vegetated areas and their condition. Eqn. 2.2 shows NDVI band ratio indices studied in this work using conventional as well as CBSI approach.

$$NDVI = \frac{\rho_{nir} - \rho_{red}}{\rho_{nir} + \rho_{red}} \tag{2.2}$$

2.2 Possibilistic Fuzzy Classifier

In this section fuzzy based classifiers have been explained and the importance of possibilistic fuzzy based classifier for extraction of single class (liquefaction) has been

discussed. One of the fuzzy based classifier fuzzy *c*-means (FCM) is a clustering technique where each data point belongs to a cluster with some degree that is specified by a membership grade and that the sum of the memberships for each pixel must be one (Bezdek, 1981, Krishnapuram and Keller, 1993). This can be achieved by minimizing the generalized least-square error objective function as Eqn. 2.3;

$$J_m(U,V) = \sum_{i=1}^{N} \sum_{j=1}^{C} (\mu_{ij})^m \left| X_i - V_j \right|_A^2 \qquad (2.3)$$

subject to constraints;

$$\sum_{j=1}^{C} \mu_{ij} = 1 \quad \text{for all i}$$

$$\sum_{i=1}^{N} \mu_{ij} > 0 \quad \text{for all j}$$

$$0 \le \mu_{ij} \ge 1 \quad \text{for all i , j}$$

and the class membership value

$$\mu_{ij} = \frac{1}{\sum_{k=1}^{c} \left(\frac{d_{ij}^2}{d_{ik}^2} \right)^{\frac{1}{(m-1)}}} \qquad (2.4)$$

where $d_{ik}^2 = \sum_{j=1}^{c} d_{ij}^2$ where X_i is the vector denoting spectral response of a pixel *i*, V_j is the mean center of a class *j*, μ_{ij} is class membership values of a pixel *i* belonging to class *j*, *c* and *N* are number of clusters and pixels respectively, *m* is a weighting exponent ($1 < m < \infty$), which controls the degree of fuzziness, $\left| X_i - V_j \right|_A^2$ is the squared distance (d_{ij}) between X_i and V_j which is given by;

$$d_{ij}^2 = \left| X_i - V_j \right|_A^2 = (X_i - V_j)^T A (X_i - V_j) \qquad (2.5)$$

where A is the weight matrix;

Amongst a number of A-norms, three namely Euclidean, Diagonal and Mahalonobis norm, each induced by specific weight matrix, are there. The formulations of each norm are given as (Bezdek, 1981);

Euclidean Norm	$A = I$	
Diagonal Norm	$A = D_j^{-1}$	(2.6)
Mahalonobis Norm	$A = C_j^{-1}$	

where I is the identity matrix, D_j is the diagonal matrix having diagonal elements as the eigen values of the variance covariance matrix, C_j given by;

$$C_j = \sum_{i=1}^{N} (X_i - V_j)(X_i - V_j)^T \tag{2.7}$$

In this study, value of weighting exponent '*m*' has been taken as 2.3 and Euclidean Norm of weight matrix '*A*' has been taken, as it gives maximum classification accuracy compared to other weighted norms and less effected with noise outlier present in training data. As Euclidean Norm uses only mean value but other norms uses mean as well as variance-covariance. Mean is less affected than variance-covariance due to the presence of noise in training data (Aziz, 2004; Kumar et al., 2006, Tso and Mather, 2009). The original FCM formulation minimizes the objective function as given in Eqn.2.3.

subject to; $$\sum_{j=1}^{C} \mu_{ij} = 1 \qquad \text{for all i}$$

While in possibilistic fuzzy classifier one would like the memberships for representative feature points to be as high as possible, while unrepresentative points should have low membership in all clusters (Krishnapuram and Keller, 1993). The objective function, which satisfies this requirement, may be formulated as;

$$J_m(U,V) = \sum_{i=1}^{N} \sum_{j=1}^{C} (\mu_{ij})^m \left| X_i - V_j \right|^2_A + \sum \eta_j \sum (1-\mu_{ij})^m \tag{2.8}$$

subject to constraints;

$$\begin{aligned} &\max_j \mu_{ij} > 0 \qquad \text{for all i} \\ &\sum_{i=1}^{N} \mu_{ij} > 0 \qquad \text{for all j} \\ &0 \le \mu_{ij} \ge 1 \qquad \text{for all i , j} \end{aligned} \tag{2.9}$$

In Eqn.2.8, η_j is a parameter that depends on the distribution of pixels in the cluster *j* and is assumed to be proportional to the mean value of the intra cluster distance. For clusters with similar distributions, η_j may be set to the same value for each cluster (Massone, et. al, 2000). Generally η_j depends on the shape and average size of the cluster *j* and its value may be computed as;

$$\eta_j = K \frac{\sum_{I=1}^{n} \mu_{ij}^m d_{ij}^2}{\sum_{i=1}^{N} \mu_{ij}^m} \tag{2.10}$$

here μ_{ij} is taken from Eqn.2.4;
where K is a constant and is generally kept a 1. The class memberships, μ_{ij}, are obtained a;

$$\mu_{ij} = \frac{1}{1+\left(\frac{d_{ij}^2}{\eta_j}\right)^{\frac{1}{(m-1)}}} \tag{2.11}$$

For extracting land cover classes, FCM is depended upon number of land cover classes to be extracted from remote sensing multi-spectral image. Membership values generated from Eqn.2.4, are depended upon summation of distances of unknown feature to mean vectors of land cover classes $(d_{ik}^2 = \sum_{j=1}^{c} d_{ij}^2)$. When extracting only one land cover class of interest, in that case $d_{ik}^2 = d_{ij}^2$ for c equals to 1 and then μ_{ij} for all features becomes one in Eqn.2.4. This concludes that all features in remote sensing multi-spectral image belong to one class, which is not the case (Tso and Mather, 2009). While working with PCM algorithm for extracting single land cover class it behaves as: $d_{ik}^2 = d_{ij}^2$, while extracting single land cover class μ_{ij}=1 for class features from Eqn.2.4 and $\sum_{i=1}^{N} \mu_{ij}^m = N$ in Eqn.2.10. So, from Eqn.2.10 $\eta_j = K \frac{\sum_{I=1}^{n} d_{ij}^2}{N}$ and from Eqn.2.11, μ_{ij} will be calculated. This indicates that possibilistic view of the membership of a feature vector in a class has nothing to do with its membership in other classes (Krishnapuram and Keller, 1993).

2.3 Entropy Analysis

Remote sensing images are attractive for the generation of land cover maps for larger areas. Assessing the accuracy of classified maps is an integral part while generating thematic classified map. The accuracy of a classification is usually assessed by comparing the classification with some reference data that is believed to accurately reflect the true land cover. As occurrence of liquefaction due to earthquake is unique activity not occurring regularly in an area. Secondly, while discriminating liquefaction areas through fraction images generated while using soft classifiers like fuzzy approaches; the fraction within pixel is not possible to locate on the ground. In this case, entropy as uncertainty indicator an absolute indirect method for accuracy assessment has been used.

The Shanon entropy (Foody, 1995) and fuzzy set based measures such as an index of fuzziness (Binaghi *et al*., 1999) may be used to estimate the uncertainty in the classification data. Entropy measures show how the strength of class membership in the classification output is partitioned between the classes for each pixel (Foody, 1996). The value of these measures is maximized (a high degree of uncertainty) when the class membership is partitioned evenly between all the classes, and minimized (a low degree or uncertainty) when the membership is associated entirely with one class. Shanon entropy, a measure conceptualized in terms of probability theory may be computed from (Klir, 1990).

$$H = -\sum_{i=1}^{c} \mu_{ij} \log_2 \left(\mu_{ij}\right) \tag{2.12}$$

where μ_{ij} denotes membership value in pixel i for class j in an image and c is the number of classes. Entropy criterion is based on actual outputs of classifier and hence is sensitive to uncertain variations. Therefore this criterion can visualize the pure uncertainty of the classification results. The uncertainty can be controlled and its effects may be mitigated by removing the uncertainty causes and reasons. The uncertainty behavior is nearly independent of the correctness behavior. The uncertainty of the classification results gives a point of view about results quality and classifier performance, where each pixel may be classified with particular uncertainty. The results extracted from Eqn.2.12 shows that the pixels are classified with different quality and certainty. Therefore the certainty criteria can be used as a new comparison means for classifier performance (Hamid and Hassan, 2006).

3. GEOLOGY AND SEISMO-TECHTONICS OF THE STUDY AREA

Different geological, seismological and hydro-logical factors could be responsible for the Bhuj earthquake-induced soil liquefaction effects. The Kachchh Peninsula forms the western most part of the Indian sub-continent. The mainland Kachchh is a peneplain and occupied by Rann of Kachchh sediments and volcanic basalts. The Kachchh region comprises of mainly Mesozoic (sandstones, siltstones, shale, and limestone), Tertiary (poorly consolidated sandstone, siltstone, and clay) and Quaternary (sand and clay) sedimentary sequences. The Kachchh seismo-tectonic belt extends approximately 250 km (East–West) and 150 km (North–South). It is flanked in the north by Nagar Parkar fault and in the south by Kathiawar fault. The area in between is traversed by several faults/fault systems. Salient among them are Katrol Hill Fault (KHF), KachchhMainland Fault (KMF), Banni Fault (BF), Island Belt Fault (IBF) and Allah Bund Fault (ABF). Geodetic measurements of plate deformation between southernmost India and the northern edge of the Gangetic Plain indicate a contraction rate of the Indian plate of 3±2 mm/yr (Paul *et al.* 2001).

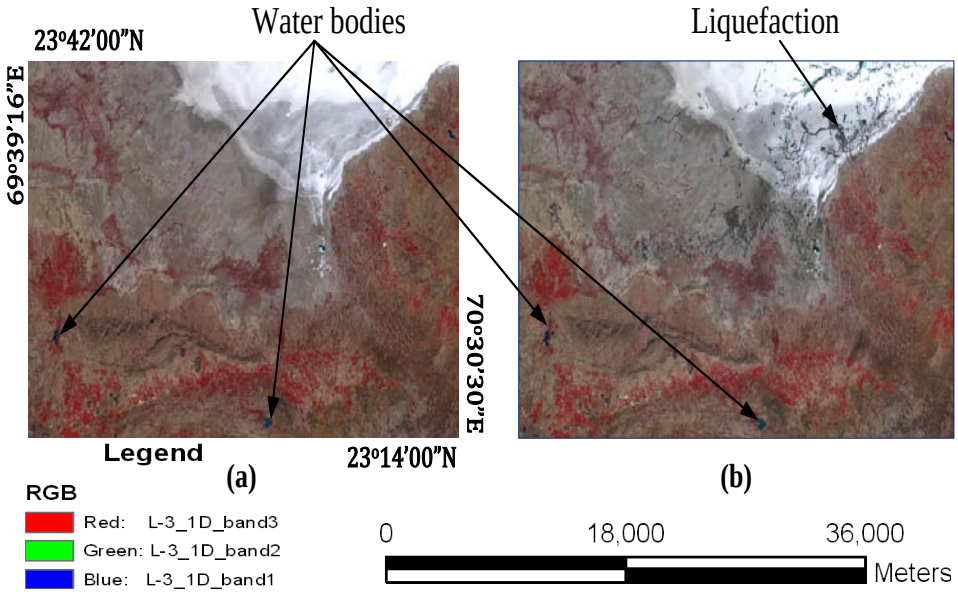

Figure 3.1. Rann of Kachchh (Study area), (a) 4th Jan, 2001, (b) 29th Jan, 2001

Test site for this work has been identified based on availability of two dates (4th Jan, 2001 and 29th Jan, 2001) IRS-1D LISS-III images. Using image processing on pre- and post- LISS III data sets it was possible to delineate precisely earthquake induced liquefaction areas indicated by liquid emanation. The LISS-III sensor carries four spectral bands green (0.52-0.59 μm), red (0.62-0.68

μm), near infrared (0.77-0.86 μm) and short-wave infrared (1.55-1.70 μm). The test site for this work has been identified as Rann of Kachchh (Lat 23°14'N-23°42'N and Long 69°39'-70°30'E) in Gujarat state of India for liquefaction identification. To separate liquefied area with pre-earthquake existing water bodies, the samples were taken from the water bodies present in this area. The 29th January, 2001 image clearly shows increased soil moisture, streams, and areas of runoff which did not exist on 4th January, 2001 as shown in Fig. 3.1(FCC image of IRS 1D having band 3,2 and 1).

4. METHODOLOGY ADOPTED

There has been requirement for identifying only one class that is, liquefaction, in Kachchh area. Keeping this in mind, the work was divided into four steps as shown in Fig. 4.1. First of all, both pre- and post-earthquake IRS-1D multispectral images (geo-referenced and atmospheric corrected) were taken. To create the models of NDVI band ratio indices, ERDAS Model Maker was used. Initially, an attempt have been made with conventional band ratio indices as per Eqn.2.2, but subsequence CBSI-NDVI band ratio indices from Eqn.2.1, was applied on study area to identify liquefaction. The fuzzy based classifier (Kumar *et al*., 2010) applied to extract single class, liquefaction as well as water bodies. The liquefaction identification and water bodies identified are shown in Fig. 5.1. At last the accuracy assessment through entropy analysis was done for both liquefaction and water body, to finalize the best result from different outputs of the indices using Eqn.2.12.

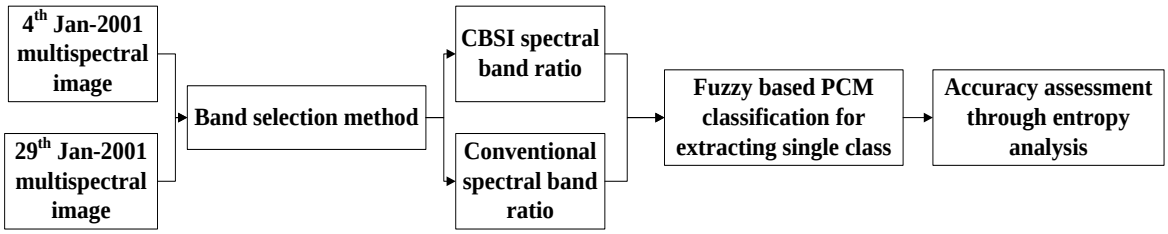

Figure 4.1. Methodology adopted

5. RESULTS AND DISCUSSION

The one class of interest, namely, liquefaction was studied for discrimination with background and especially separates it with pre earthquake existing water bodies in the study area. NDVI indices help to distinguish reflectance of soils by its moisture content. The NDVI band ratio technique was applied on both images using CBSI as well as spectral band ratio approach to find out liquefaction and water bodies. Table 5.1 shows temporal indices value and indicate that CBSI-NDVI approach give less correlation (as degree of belongingness to a class) for liquefaction identification, means it can better separate one class of interest with other classes. As water bodies not changed in this period therefore the temporal indices values for water bodies not changed very much. For water bodies identification it is observed from Table 5.1 that both temporal indices shows high correlation in both temporal data, means not much variation in indices values in between these two dates.

Table 5.2 shows that liquefaction and water body identified with less entropy using CBSI approach, means the CBSI approach can better reduce the uncertainty in the respective class. The minimum membership value to represent the output of liquefaction is also less in case of CBSI but in case of water body identification the conventional temporal indices with minimum membership value (0.98) give better result to represent the output.

Table 5.1. Indices values for liquefaction and water body identification

Liquefaction				Water body			
CBSI-Indices		Conventional-Indices		CBSI-Indices		Conventional-Indices	
Membership value range	Entropy	Membership value range	Entropy	Membership value range	Entropy	Membership value range	Entropy
0.956-0.996	0.005	0.929-0.996	0.011	0.956-0.996	0.005	0.956-0.996	0.011

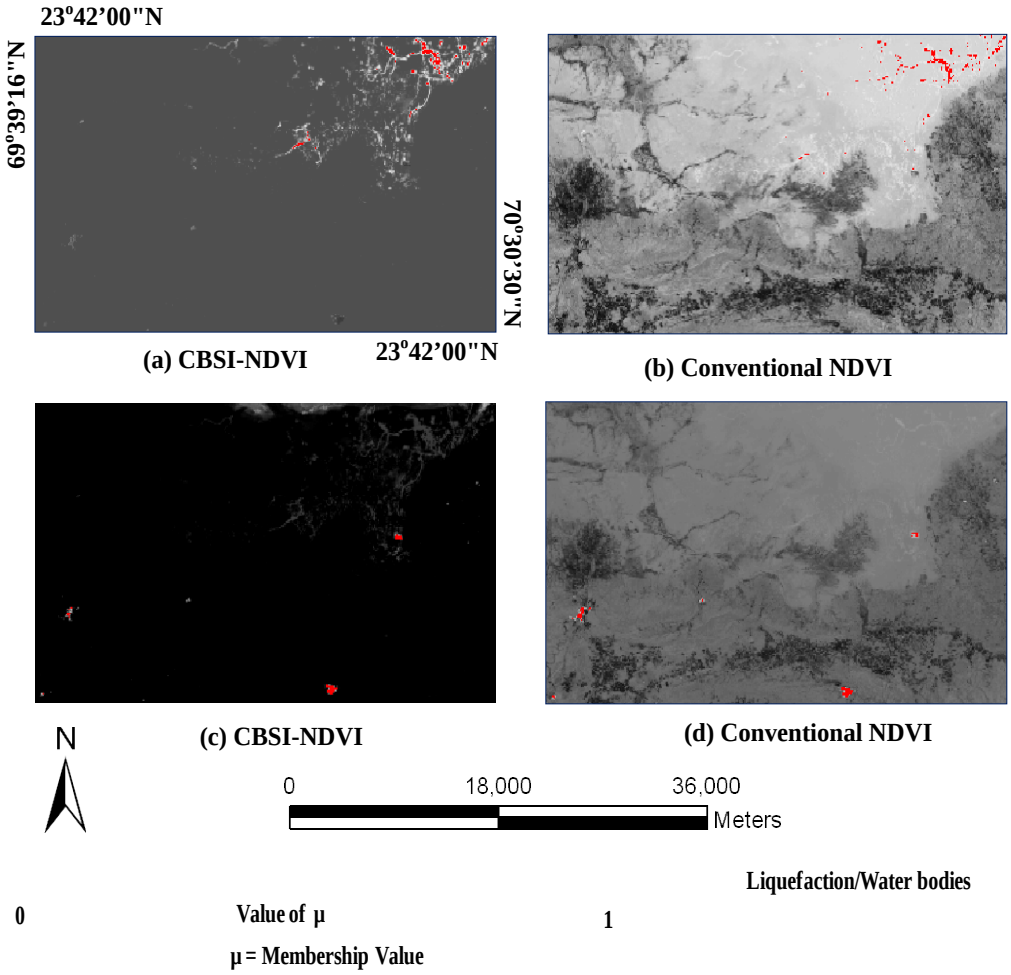

Figure 5.1. Classified outputs (a) CBSI-NDVI liquefaction output (b) Conventional NDVI liquefaction output (c) CBSI-NDVI water bodies output (d) Conventional NDVI water bodies output

In the study area at the time of rainy season, the ground is filled up with water and during the dry season, the water evaporates and the salt in the water spreads on the surface of the earth. Therefore, due to the influence of salt, the soil at Kachchh region depicts different reflectance. The NDVI based on CBSI and conventional approach have been generated as shown in Fig. 5.1. In these images both water bodies and liquefaction areas have high membership values and seen as bright area. The result clearly indicates that one class of interest (liquefaction) not mixed with other class (water bodies). From Table 5.2 and Fig. 5.1, it is clear that CBSI approach give better results with less entropy and better output, as compare to conventional one. It is observed that for liquefaction areas CBSI-NDVI shows good matching to PCM results. When the entropy values for water bodies and liquefied areas are computed (Table 5.2), it is found that it has

low values. It means the one class of interest (liquefaction) is better separate with other class (water bodies).

Table 5.2. Membership range and Entropy of different Indices for liquefaction and water body identification

Liquefaction				Water body			
CBSI-Temporal Indices		Conventional-Temporal Indices		CBSI-Temporal Indices		Conventional-Temporal Indices	
4^{th}Jan	29^{th} Jan	4^{th} Jan	29^{th} Jan	4^{th}Jan	29^{th} Jan	4^{th} Jan	29^{th} Jan
0	0.549	0.388	0.321	0.749	0.745	0.176	0.180

6. CONCLUSION

In this study, effect of NDVI indices (CBSI and conventional) has been studied for extracting liquefaction as well as water bodies in the study area. It is observed that with better separability, less entropy and less membership range, the CBSI technique give better results to identify liquefaction. For water body identification CBSI approach also shows better separability, less entropy with same membership range. Therefore CBSI technique overall performed better results as compare to conventional technique. Overall CBSI-NDVI is best for both water bodies and liquefaction identification. The methodology proposed in this work requires minimal reference data for training sample and less information requirement about image characteristics for identification liquefaction and water bodies. This methodology provides a quick and efficient way to classify liquefaction locations and may be useful for management and development plans for decision makers, local administrations, and scientists interested in liquefaction.

REFERENCES

Arora, M.K., Das Gupta, A.S. and Gupta, R.P. (2004). An artificial neural network approach for landslide hazard zonation in the Bhagirathi (Ganga) Valley, Himalayas. *International Journal of Remote Sensing* **25:3**, 559–572.

Aziz, M.A. (2004). Evaluation of soft classifiers for remote sensing data. Unpublished *Ph.D thesis*, IIT Roorkee, Roorkee, India.

Baraldi, A. and Parmiggiani, F. (1995). A neural network for unsupervised categorization of multivalued input patterns: an application to satellite image clustering. *IEEE Transactions on Geoscience Remote Sensing* **33:2**, 305–316.

Bastin, L. (1997). Comparison of fuzzy C-means classification, linear mixture modeling and MLC probabilities as tools for unmixing course pixels. *International Journal of Remote Sensing* **18**, 3629–3648.

Bezdek, J.C. (1981). Pattern Recognition with Fuzzy Objective Function Algorithm. Plenum, New York, USA.

Binaghi, E., Brivio, P.A., Chessi, P. and Rampini, A. (1999). A fuzzy Set based Accuracy Assessment of Soft Classification. *Pattern Recognition letters* **20**, 935-948.

Foody, G.M. (1995), "Cross-entropy for the evaluation of the accuracy of a fuzzy land cover lassification with fuzzy ground data", *ISPRS Journal of Photogrammetry and Remote Sensing*, **50**, 2–12.

Foody, G.M. (1996), "Approaches for the production and evaluation of fuzzy land cover classifications from remotely sensed data", *International Journal of Remote Sensing*, **17**, 1317–1340.

Gupta, R. P., Saraf, A. K., and Chander, R. (1998). Discrimination of areas susceptible to earthquake-induced liquefaction from Landsat data. *International Journal of Remote Sensing* **19**, 569–572.

Hamid, D. and Hassan, G. (2006). Measurement of uncertainty by the entropy: application to the classification of MSS data. *International Journal of Remote Sensing* **27:18**, 4005-4014.

Hansen, M.C., Defries, R.S., Townshend, J.R.G. and Sohlberg, R. (2000). Global land cover classification at 1 km spatial resolution using a classification tree approach. *International Journal of Remote Sensing* **21**, 1331–1364.

Klir, G.J. (1990). A principle of uncertainty and information variance. *International Journal of General Systems* **17**, 249–275.

Krishnapuram, R. and Keller J.M. (1993). A possiblistic approach to clustering. *IEEE Transactions on Fuzzy Systems* **1**, 98–108.

Kumar, A., Ghosh, S.K. and Dadhwal, V.K. (2006). Sub-Pixel Land Cover Mapping: SMIC System. *ISPRS* International Symposium on *"Geospatial Databases for Sustainable Development"* Goa, India, September 27-30.

Kumar, A., Ghosh, S.K. and Dadhwal, V.K. (2010). ALCM:Automatic land cover mapping. *Journal of Indian remote sensing* **38**, 239-245.

Lucas, R., Rowlands, A., Brown, A., Keyworth, S. and Bunting, P. (2007). Rule-based classification of multi-temporal satellite imagery for habitat and agricultural land cover mapping. *ISPRS Journal of photogrammetry and Remote Sensing* **62:3**, 165-185.

Malik, J.N., Sohoni, P.S., Karanth, R.V. and Merh, S.S. (1999). Modern and historic seismicity of Kachchh Peninsula, Western India. *Journal of the Geological Society of India* **54**, 545–550.

Massone, A. M., Masulli, F. and Petrosino, A. (2000), Fuzzy clustering algorithms on Landsat images for detection of waste areas: a comparison, in Advances in Fuzzy Systems and Intelligent Technologies, (eds.) F. Masulli, R. Parenti and G. Pasi, Shaker, Maastricht, NL, 165-175.

Matsakis, P., Andrefouet, S. and Capolsini, P. (2000). Evaluation of fuzzy partitions. *Remote Sensing of Environment* **74**, 516–533.

Pal, M. and Mather, P.M. (2003). An assessment of the effectiveness of decision tree methods for land cover classification. *Remote Sensing of Environment* **86**, 554–565.

Paul, J., Burgmann, R., Gaur, V. K., Bilham, R., Larson, K. M., Ananda, M. B., Jade, S., Mukal, M., Anupama, T. S., Satyal, G. and Kumar, D. (2001). The motion and active deformation of India. *Geophysical Research Letters* **28:4**, 647-651.

Ramakrishnan, D., Mohanty, K.K. and Nayak, S.R. (2006). Mapping the liquefaction induced soil moisture changes using remote sensing technique: an attempt to map the earthquake induced liquefaction around Bhuj, Gujarat, India. *Geotechnical and Geological Engineering* **24**, 1581–1602.

Rouse, J.W., Haas, R.H., Schell, J.A., and Deering, D.W., (1973). Monitoring vegetation systems in the Great Plains with ERTS. *Third ERTS Symposium, NASA* SP-**351:I**, 309-317.

Saraf, A.K., Sinvhal, A., Sinvhal, H., Ghosh, P. and Sarma, B. (2002). Satellite data reveals 26 January 2001 Kutch Earthquake induced ground changes and appearance of water bodies. *International Journal of Remote Sensing*. **23:9**, 1749–1756.

Tso, B. and Mather, P. M. (2009). *Classification Methods for Remotely Sensed Data.* CRC Press, Boca Raton, 56 and 69.

Wardlow, B.D. and Egbert, S.L. (2008). Large-area crop mapping using time series MODIS 250 m NDVI data, An assessment for the U.S. Central Great Plains. *Remote Sensing of Environment* **112**, 1096–1116.